27th ABCM International Congress of Mechanical Engineering
December 04-08, 2023, Florianópolis-SC, Brazil

COB-2023-2215
THERMODYNAMIC ANALYSIS OF A POLYGENERATION PLANT BASED ON LNG-REGASIFICATION FOR CO_2 CAPTURE AND AIR LIQUID STORAGE

Pedro Otávio de Carvalho Ramos
José Vicente Hallak Dangelo
University of Campinas – 500 Albert Einstein Avenue, School of Chemical Engineering – Campinas/SP – Brazil – CEP: 13083-852
e-mails: pedrootaviocr24@gmail.com, dangelo@unicamp.br

Abstract. *Due to its cryogenic temperature, liquefied natural gas (LNG) has a great potential to act as a cold source in thermal systems. Among other applications, the cold from LNG regasification can be used to capture CO_2 from flue gas and to store energy in the form of liquid air. The reduction of CO_2 emissions is increasingly urgent given the concern about global warming, while the technology of energy storage in liquid air presents itself as an excellent source of energy, which can be released according to the demand, having a high efficiency when the process is integrated with an LNG regasification plant. This work analyzes the thermodynamic performance of an integrated system in which the cold from LNG regasification process is used for both energy storage in liquid air and for capturing CO_2 from a flue gas stream. Simulations of the proposed system were performed using Aspen HYSYS® software. Parametric analyses were conducted to investigate the effect of the key variables on the energetic and exergetic efficiencies of the system, which were than optimized. The results obtained for the round-trip and exergetic efficiencies of the energy storage subsystem, and for the net electrical and exergetic efficiencies of the Allam cycle were respectively: 125,93%, 71,50%, 79,37% and 57,42%.*

Keywords: *LNG regasification, carbon dioxide capture, flue gas, liquid air, simulations.*

1. INTRODUCTION

Climate change caused by the emission of greenhouse gases has become an increasingly worrying issue for mankind in recent years. In the current scenario, the burning of fossil fuels in thermoelectric plants is responsible for most of the global CO_2 emissions into the atmosphere (around 40%), as illustrated in Figure 1, contributing to the greenhouse effect and, consequently, to global warming.

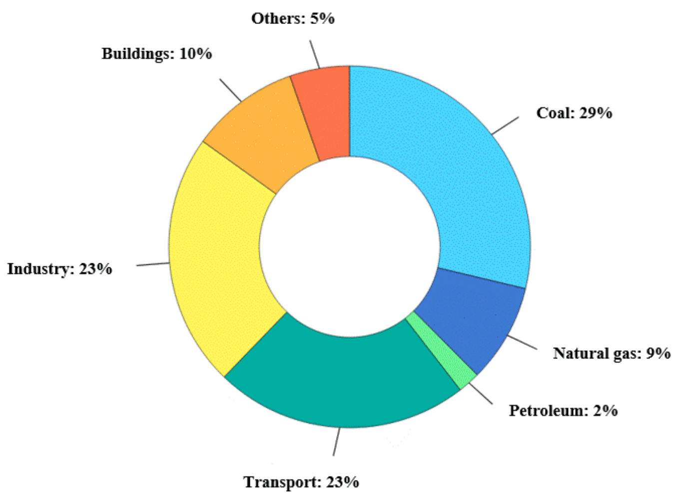

Figure 1. Distribution of global sources of CO_2 emissions in the atmosphere (IEA, 2022).

A measure of the countries concern with the impacts caused by the emission of greenhouse gases is evidenced by the Paris Agreement, signed by 196 countries on December 12, 2015, at the 21st Climate Conference (COP-21) in Paris and some key aspects of this Agreement rely on "seeking to strengthen the global response to climate change limiting global temperature increase below 2 °C" compared to pre-industrial levels and "reduce greenhouse gas emissions by at least 40% until 2030 compared to 1990". Brazil has committed to reduce its greenhouse gas emissions by 37% by 2025 compared to the levels emitted in 2005, raising this target to 43% by 2030 (Meireles, 2020).

Among fossil fuels, natural gas is the one with the lowest rate of greenhouse gas emissions. The uneven distribution of its reserves is a limited factor for its transportation. To overcome this problem, natural gas is converted to liquid form (liquefied natural gas, or LNG), which has a volume approximately 600 times smaller than natural gas in the gas phase. The very low temperature of LNG (around -162 ºC) makes it a potential source to extract heat, which will be referenced in this work with an expression commonly used in LNG studies, which is "cold energy". After transport and before being used by final consumers, LNG must undergo a regasification process during which, generally, there is a great waste of cold energy (Atienza-Marquez et al., 2018).

Due to its cryogenic temperature, liquefied natural gas (LNG) has a great potential to act as a cold source in thermal systems. Among other applications, the cold from LNG regasification can be used to capture CO_2 from flue gas and to store energy in the form of liquid air. The reduction of CO_2 emissions is increasingly urgent given the concern about global warming, while the technology of energy storage in liquid air presents itself as an excellent source of energy, which can be released according to the demand, having a high efficiency when the process is integrated with an LNG regasification plant. Therefore, it is noted that the LNG regasification process presents a great opportunity to use cold energy and among several applications for this cold energy source there are two of great importance: CO_2 capture and liquid air energy storage

A cryogenic energy storage system can be seen in an even more positive way if CO_2 capture is present in the process. CO_2 is one of the greatest contributors to the greenhouse effect and its emissions come mainly from the burning of fossil fuels. For electricity generation from fossil fuels, the oxy-fuel combustion process is very promising for CO_2 capture. Such a process requires virtually pure oxygen, which can come from an air separation process. In this context, this CO_2 from an oxy-fuel combustion process can be captured after water is condensed from the stream using a cryogenic energy system, since this has a relatively large amount of cold energy (Li et al., 2011).

Considering a global scenario of increasing LNG production, it is very important that its potential as a cold source can be optimized. A polygeneration plant presents itself as a very interesting option for the production of electricity, CO_2 capture and supply of regasified natural gas ready for transport and use by final consumers. Such a plant can be configured with an energy integration between the following processes: LNG regasification, CO_2 capture and liquid air storage. Furthermore, an organic Rankine cycle can be coupled to the LNG regasification process so that cold energy waste is avoided, and higher energy storage performance is achieved (Yu et al., 2021).

The objective of this work is to perform a thermodynamic analysis of a polygeneration plant based on simulations of the three processes mentioned, considering parametric analyses to investigate the effect of the key operational variables on the energetic and exergetic efficiencies of the system and based on them an optimization procedure was used to maximize these efficiencies.

2. SYSTEM DESCRIPTION

The schematic diagrams of the proposed polygeneration plant are presented in Figures 2 to 7. The subsystems proposed are not new and were taken from the literature (Atienza-Márques, 2018 and Chan et al., 2019). The novelty of this work is the attempt to integrate the individual systems, to increase the efficiency of the polygeneration plant. The fragmentation of the system into several figures was carried out in order to present the system in detail and with a greater clarity. In Figure 2, there are four subflowcharts, which are detailed in Figures 3 to 6, respectively.

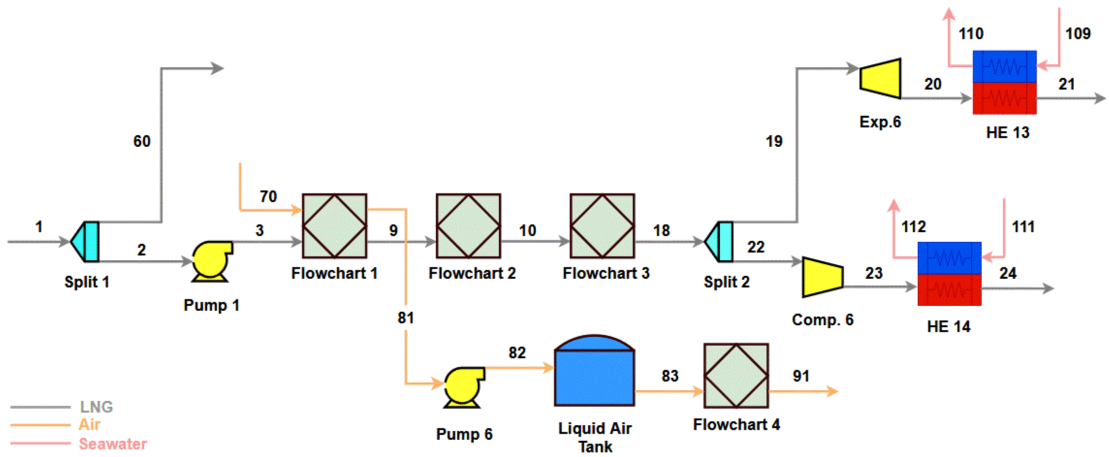

Figure 2. Condensed diagram of the polygeneration plant.

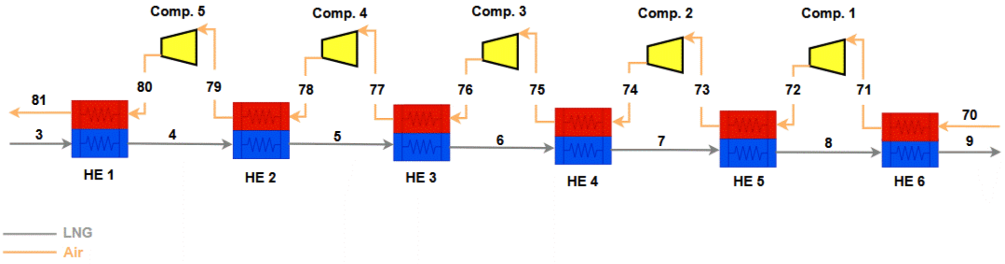

Figure 3. Flowchart 1 - Air liquefaction process.

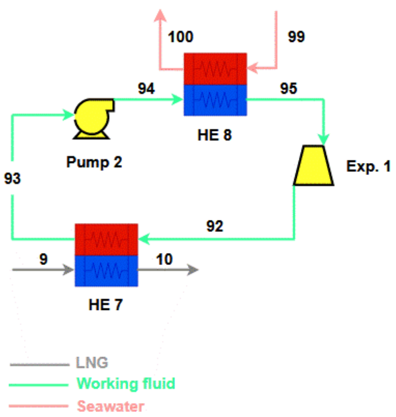

Figure 4. Flowchart 2 - Organic Rankine cycle.

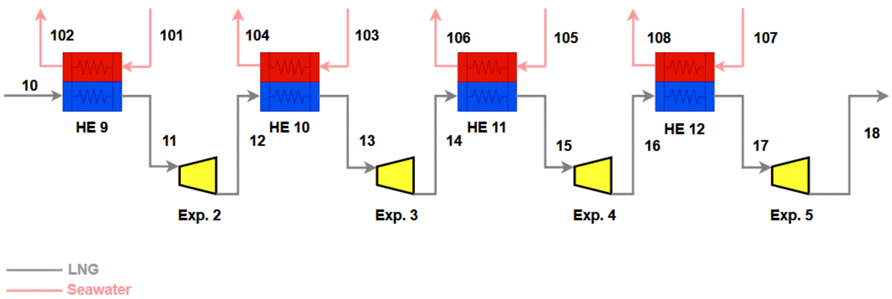

Figure 5. Flowchart 3 – LNG regasification (heating and expansion) process.

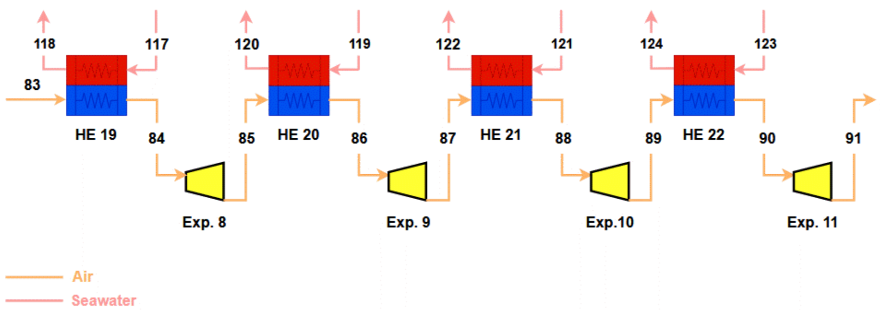

Figure 6. Flowchart 4 – Air heating and expansion process.

Stream #1 of liquefied natural gas, with a mass flow rate of 97.5 kg/s (100% CH_4), at -162 ºC and 1.3 bar, is divided into two: stream #2, 10 kg/s, which is used to exchange heat with an air stream in order to liquefy it, while the remaining

87.5 kg/s (stream #60) is used to cool a flue gas stream so that it is possible to perform the separation of CO_2 and H_2O. Stream #2 is pumped up to a pressure of 300 bar and is then heated by successive heat exchangers in countercurrent with air. Then, gaseous stream #9 of natural gas at a temperature of -59 ºC exchanges heat with the working fluid of an organic Rankine cycle and reaches a temperature of -25 ºC (stream #10). Finally, natural gas performs successive heat exchanges with seawater and expansions, reaching after the last turbine, a temperature of 0.65 ºC and a pressure of 84.90 bar (stream #18).

Stream #18 is split in two fractions, 90% (stream #19) are sent to a network of final consumers, while the remaining 10% (stream 22#) continues in the process, subsequently undergoing a compression to 306 bar and exchanges heat with a sea water stream (stream #11) up to 51.01 ºC (stream #24). This stream then joins stream #69 of recirculating natural gas and a mass flow rate of 1 kg/s, under the same temperature and pressure, which originates from stream #60. Stream #25, natural gas and mass flow rate of 2 kg/s, goes to a combustion chamber where it finds stream #52 of recirculating CO_2 and stream #59 composed of a mixture of recirculating CO_2 and O_2. The amount of O_2 was defined so that oxy-fuel combustion was practically complete in the chamber, with the main combustion products being CO_2 and H_2O.

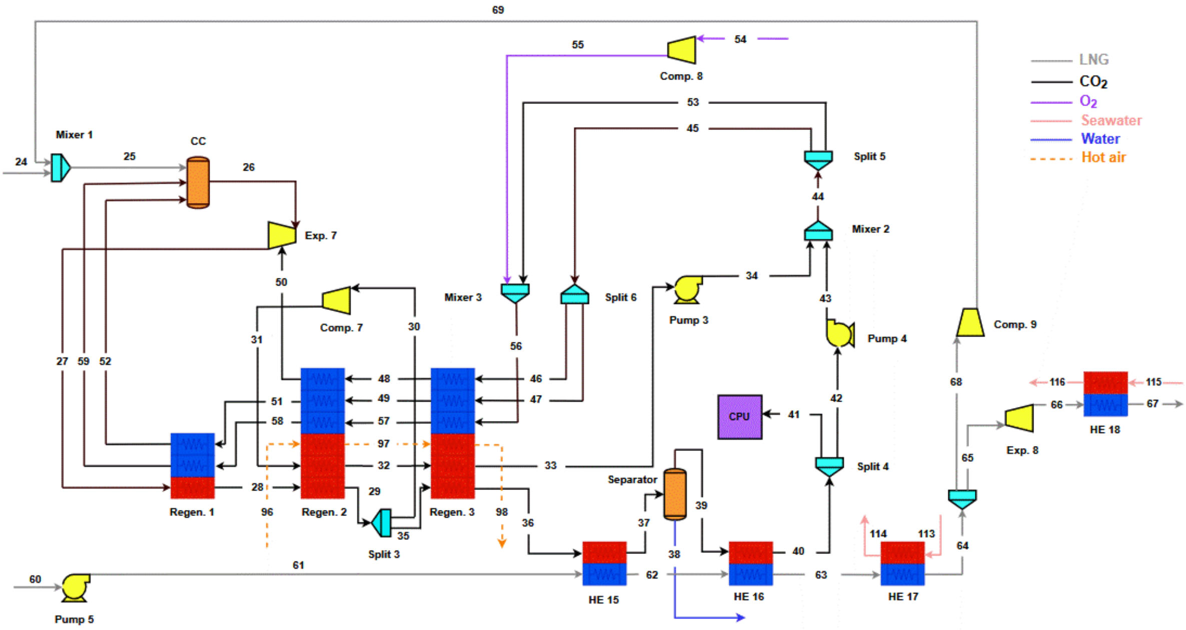

Figure 7. Flowchart of the oxy-fuel combustion of natural gas and CO2 capture process.

Stream #26, from the combustion chamber, undergoes an expansion, which is modeled in the simulation by the continuous expansion model of El Masri (Chan et al., 2019). In this model, the expansion process is divided into N + 1 subturbines. The discharge from the first turbine is cooled by mixing with a stream of recycled flue gas, while the discharge from the last subturbine is not cooled. The pressure ratio for the first subturbine was set at 0.903, and its calculation was performed iteratively and the inlet temperature of the last subturbine was set at 860 ºC (permissible by the turbine blade). The number of turbines was set to be 15 to ensure model efficiency (Chan et al., 2019).

After expansion, the flue gas stream #27 passes through a sequence of three regenerators in series in countercurrent with recycle streams. Since the heat capacity of the low pressure flue gas stream is lower than that of the high pressure recycle streams, there is an imbalance between the heat released by the flue gas and the heat required to raise the temperature of the recycle stream to the required level. Thus, in order to avoid a temperature cross, stream #96 of hot air is supplied to regenerator 2, and 9.1% of the partially cooled flue gas (stream #30) is extracted at 130.4 °C from the outlet of the regenerator 2 and adiabatically compressed to 232.8°C and 90 bar in a bypass compressor.

Stream #36 with most of the flue gas leaving regenerator 3 then goes to a heat exchanger, cooling to 2 ºC and consequent water condensation. After this process, stream #37 has a CO_2 content of 91.86% and enters a separator so that the condensed water (stream 38) is separated. The output stream (stream 39) has its CO_2 content raised to 0.9866, and goes to another heat exchanger, where it is cooled to -11.80 ºC. Then stream #40 is split into stream #42 (3.6%) that is sent to a CO_2 processing unit for capture while the remaining and stream #42 (96.4%) which continues through the process, being pumped to 306 bar. Then there is a mixture with stream #34 of flue gas from the bypass, which gives off heat in regenerator 3 and is pumped up to a pressure of 306 bar. The resulting stream is divided into three streams: stream #46 is directed to the discharge of the subturbines of the continuous expansion model of El Masri after being heated in regenerators 3 and 2, respectively; stream #47 feeds the combustion chamber after passing through the three regenerators; and stream #53 is mixed with stream #55 of practically pure O_2 and also goes to the combustion chamber after being heated by the three regenerators. The streams that enter the heat exchangers HE15 and HE16, in countercurrent, cooling the flue gas are the 87.5 kg/s of liquefied natural gas originating from the initial stream (stream #60). After the second heat exchanger, stream #63, of natural gas, is heated in a heat exchanger in countercurrent with sea water up to 10 ºC. It is then divided into two streams: stream #65 with a mass flow rate of 86.5 kg/s, that is sent to final gas consumers and stream #68, 1 kg/s, that expands to 306 bar before joining, under the same temperature and pressure conditions, to the portion of 1 kg/s (stream #22) from the 10 kg/s stream of natural gas.

3. METHODOLOGY

Considering the objective of this work which is to perform a thermodynamic analysis of a polygeneration system that uses cold energy from the LNG regasification process to capture CO_2 and store energy in liquid air, it is important to mention that, in the open literature, most works consider these applications individually. To integrate them a simulation of the polygeneration plant was implemented using Aspen HYSYS® v. 10 simulator. The most suitable choice for the thermodynamic package for this system is the Peng-Robinson equation of state, as it is recommended for hydrocarbons and other nonpolar substances.

For system modeling, some assumptions are made, such as: system operation is under steady-state conditions; variations of kinetic and potential energies are neglected; pressure drops in system components (except pumps, compressors, turbines and valves) and in piping are neglected as well; all equipment were considered adiabatic; the isentropic efficiency of turbines, pumps and compressors are assumed to be constant.

To evaluate the thermodynamic performance of the polygeneration plan some parameters were considered in the two subsystems studied. For the liquid air energy storage subsystem, the parameters calculated were round-trip efficiency and exergetic efficiency and for the oxy-combustion subsystem (Allam cycle), the parameters were net electrical efficiency and exergetic efficiency.

Round-trip efficiency is the most important parameter used to evaluate the performance of energy storage systems. It is defined as the difference between the power produced by the energy release mode and the power produced by the conventional mode of operation, divided by the power required by the energy storage mode (Lee and You, 2019). The round-trip efficiency, which is given by Eq. (1), was calculated based on the part of the system corresponding to energy storage in liquid air, as this definition only makes sense for energy storage systems. For this purpose, streams #2 to #18 were considered for natural gas, and streams #70 to #91 for air.

$$\eta_{RT} = \frac{\dot{W}^{rls} - \dot{W}^{cnv}}{\dot{W}^{stg}} \tag{1}$$

where η_{RT}, $\dot{W}^{rls}$, $\dot{W}^{cnv}$ and $\dot{W}^{stg}$ are the round-trip efficiency of an energy storage system, power produced by the energy release mode, power produced by the conventional energy mode and energy required by the storage mode, respectively.

The net electrical efficiency of an Allam cycle is defined as the ratio between the net output power of the cycle and the product of the mass flow rate of the fuel to be burned by its lower heating value (Chan et al., 2019). The net electrical efficiency, given by Eq. (2), was calculated considering the part of the system corresponding to the Allam cycle (Figure 7), as it is defined in relation to the mass flow rate that enters the combustion chamber.

$$\eta_{el} = \frac{\dot{W}_{net}}{\dot{m}_{fuel}\ x\ LHV} \tag{2}$$

where η_{el}, $\dot{W}_{net}$, $\dot{m}_{fuel}$ and LHV are the net electrical energy efficiency of an Allam cycle, net power output, mass flow rate of natural gas for combustion and lower heating value, respectively.

The exergetic efficiency of a system is defined in different ways in the literature, according to its configuration and purpose. Considering an energy storage system, Lee and You (2019) defined exergetic efficiency as the ratio between the output net exergy rate and the input net exergy rate, as show in Eq. (3).

$$\eta_{Exg1} = \frac{E\dot{x}g_{net,out}}{E\dot{x}g_{net,in}} \tag{3}$$

where η_{Exg1}, $E\dot{x}g_{net,out}$ and $E\dot{x}g_{net,in}$ are the exergetic efficiency, net exergy output and net exergy input of the energy storage system, respectively.

For an Allam cycle, Chan et al. (2021) defined exergetic efficiency as the following ratio: the sum of the net power output module and cooling exergy output of the system by the sum of the fuel exergy available for combustion and the natural gas net cold exergy input.

$$\eta_{Exg2} = \frac{|\dot{W}_{net}| + E\dot{x}g_c}{E\dot{x}g_i} \tag{4}$$

where η_{Exg2}, $\dot{W}_{net}$, $\dot{Exg}_c$ and $\dot{Exg}_i$ are the exergetic efficiency of the Allam cycle, net power output, cooling exergy output and sum of fuel exergy for combustion and LNG net cold exergy input.

4. RESULTS AND DISCUSSION

4.1 Parametric analysis

After validation of all subsystems that compose the polygeneration plant, using data from the literature, a parametric analysis was carried out in order to define the ranges of the main operating variables that could be used in a following optimization procedure. The analyses were conducted considering the impact of different variables on system efficiencies, keeping all others constant.

Figure 8 shows the influence of the LNG pump discharge pressure (stream #3) on the return efficiency of the energy storage subsystem considering a range of pressures from 292 to 320 bar. This range was chosen because values below 292 bar and above 320 bar generate convergence problems in the system. It can be noted that the round-trip efficiency for the energy storage system decreases linearly, with the highest value equal to 125.93% obtained using a pressure of 292 bar (it is important to mention that round-trip efficiency can be greater than 100% considering the way it is defined).

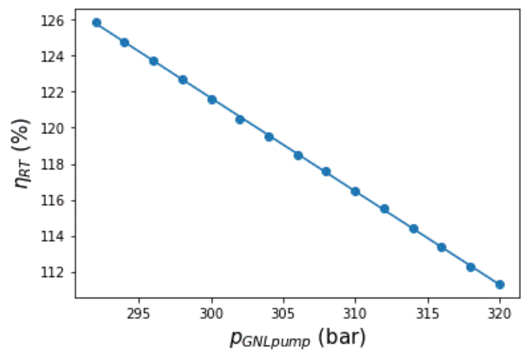

Figure 8. Round-trip efficiency as a function of LNG pump discharge pressure.

Figure 9 shows the influence of the mass flow rate of the bypass current (current #30) on the net electrical efficiency of the Allam cycle. It can be seen that it decreases linearly with the increase in the mass flow rate in the range from 0 to 20 kg/s. In other words, the absence of bypass current causes the net electrical efficiency to be maximum, in contrast to what was obtained by Chan et al. (2021). Thus, considering that the process simulation has used a mass flow rate of 15.13 kg/s, removing the bypass would imply in an increase of the efficiency without prejudice to the heat exchange process in regenerators 2 and 3.

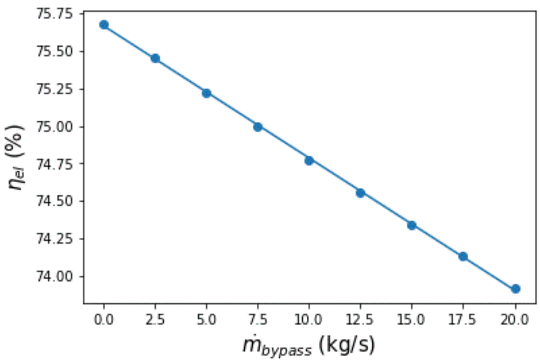

Figure 9. Net electrical efficiency of the Allam cycle as a function of bypass stream mass flow rate.

Figure 10 shows the influence of the gas turbine discharge pressure (stream #27) on the electrical efficiency of the Allam cycle considering a range of pressures from 30.5 to 35 bar. This interval was chosen because values below 30.5 bar and above 35 bar generate convergence problems in the system. It can be seen that the net electrical efficiency of the Allam cycle decreases linearly, with the highest value equal to 77.35% obtained using a pressure of 30.5 bar. Therefore, the efficiency of the process can be increased by reducing the turbine discharge pressure, since the pressure used in the simulation was 34 bar.

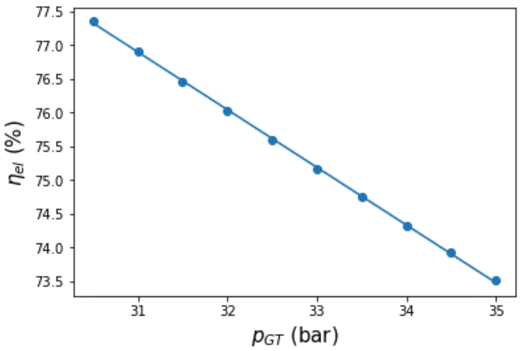

Figure 10. Net electrical efficiency of the Allam cycle as a function of gas turbine discharge pressure.

Figure 11 shows the influence of the LNG mass flow rate (stream #1) on the net electrical efficiency of the Allam cycle considering an interval with flow values from 90 to 104 kg/s. Note that the net electrical efficiency grows linearly and it is not so much influenced by the mass flow rate. An increase of approximately 16% of the mass flow rate causes an increase of only 0.5% of the net electrical efficiency.

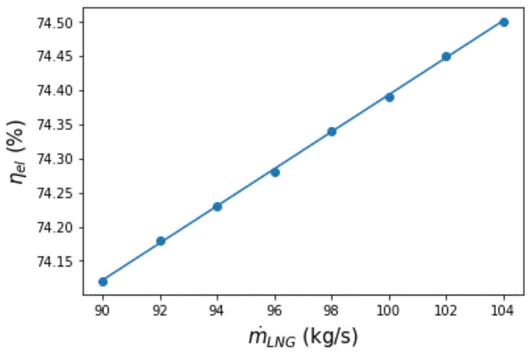

Figure 11. Net electrical efficiency of the Allam cycle as a function of LNG mass flow.

Figure 12 presents the influence of the maximum pressure of the oxyfuel cycle (stream #44) on the electrical efficiency of the Allam cycle considering a pressure range from 216 to 306 bar. This interval was chosen because values below 216 bar and above 306 bar have shown not to be feasible. It is noticed that the net electrical efficiency of the Allam cycle reaches a local maximum around 276 bar. In this way, the efficiency of the process can be increased by reducing the maximum pressure of the oxyfuel cycle, since the pressure used in the simulation was 306 bar.

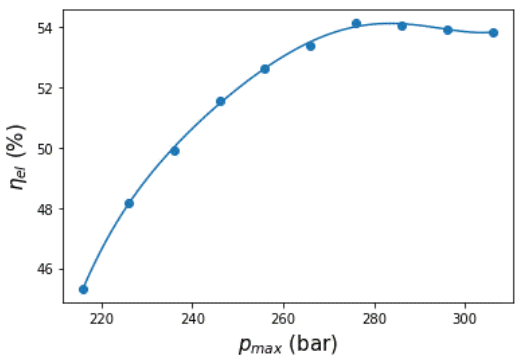

Figure 12. Net electrical efficiency of the Allam cycle as a function of maximum pressure of the Allam cycle.

4.2 Optimization

To optimize the system efficiencies, Aspen HYSYS® optimizer tool was used. It allows optimizing the operation of a process unit, seeking to maximize or minimize a specific objective function, according to certain criteria. Advanced algorithms are used to explore different configurations of process variables such as mass flow rates, temperatures and pressures. They are adjusted in successive iterations, in order to find the best configuration that meets the defined criteria. The optimizer also considers process constraints such as temperature, pressure, and mass flow limit and takes into account mass and energy balance equations. The optimizer provides the optimal configuration of the process, along with the values of the variables that achieve the desired goals. In order to optimize the process efficiencies, the objective function given by Eq. (5) was maximized. The input variables and their ranges can be found in Table 1.

$$\text{Obj} = \eta_{RT} + \eta_{Exg1} + \eta_{electrical\_net} + \eta_{Exg2} \quad (5)$$

where η_{RT}, η_{Exg1}, $\eta_{electrical\_net}$ and η_{Exg2} are the round-trip efficiency for the energy storage system, exergetic efficiency for the energy storage system, net electrical efficiency for the Allam cycle and exergetic efficiency for the Allam cycle, respectively.

Table 1. Input variables and their ranges.

Operating variable	**Range**
LNG pump discharge pressure (stream #3), bar	292-320
Bypass stream mass flow (stream #30), kg/s	0-20
Oxy-combustion cycle gas turbine discharge pressure (stream #27), bar	30.5-35
LNG mass flow (stream #1)	90-104
Oxy-combustion cycle maximum pressure (stream #44), bar	216-316

In the initial simulation of the process, the value found for the objective function was 321.1. After optimization, a value of 334.2 was found, indicating that the system efficiencies could be improved by modifying process variables. For this optimal value of the objective function, the results obtained for the input variables and for the system efficiencies are illustrated in Tables 2 and 3.

Table 2. Optimized values of the operating variables.

Operating variable	**Result**
LNG pump discharge pressure (stream 3), bar	292
Bypass stream mass flow (stream 30), kg/s	0
Oxy-combustion cycle gas turbine discharge pressure (stream 27), bar	30.5
LNG mass flow (stream 1)	96.80
Oxy-combustion cycle maximum pressure (stream 44), bar	276

Table 3. Optimized values of the efficiencies.

Efficiency	**Result**
Round-trip efficiency for the energy storage subsystem, %	125.93
Exergetic efficiency for the energy storage subsystem, %	71.50
Net electrical efficiency for the Allam cycle, %	79.37
Exergetic efficiency for the Allam cycle, %	57.42

5. CONCLUSION

An integrated system in which the cold from the LNG regasification process is used both for energy storage in liquid air and for capturing CO_2 from flue gas was simulated in Aspen HYSYS® software. Parametric analyses were conducted to investigate the effect of operational variables on the efficiencies of the system and an optimization was performed using Aspen HYSYS® optimizer tool.

The optimal values of the round-trip efficiency for the energy storage subsystem, exergetic efficiency for the energy storage subsystem, net electrical efficiency for the Allam cycle and exergetic efficiency for the Allam cycle were 125.93%, 71.50%, 79.37% and 57.42%, respectively.

The integration of both energy storage liquid air system and CO_2 capture system with an LNG regasification process has shown to be feasible and this integrated polygeneration plant has a great potential to maximize the efficiencies of the individual subsystems. A further economic analysis will help to establish its viability.

6. ACKNOWLEDGEMENTS

The authors are grateful for the financial support of the Human Resources Program for the Oil and Gas Sector of the National Agency of Petroleum, Natural Gas and Biofuels – PRH-ANP.

7. REFERENCES

Atienza-Márquez, A., Bruno, J. C. and Coronas, A., 2018. “Cold recovery from LNG-regasification for polygeneration applications”. *Applied Thermal* Engineering, Vol. 132, p. 463-478.

Chan, W., Li, H., Chang, F., Wang L. and FENG, Z., 2021. “Exergoeconomic analysis and optimization of the Allam cycle with liquefied natural gas cold exergy utilization”. *Energy Conversion and Management*, Vol. 235.

IEA, 2022, *Global energy-related CO_2 emissions by sector*, International Energy Agency IEA, Paris, https://www.iea.org/data-and-statistics/charts/global-energy-related-co2-emissions-by-sector. Accessed 07 September 2022.

Lee, I. and You, F, 2019. “Systems design and analysis of liquid air energy storage from liquefied natural gas energy storage”. *Applied Energy*, Vol. 242, p. 168-180.

Li, Y., JIN, Y., CHEN, H. TAN, C. and DING, Y. “An integrated system for thermal power generation, electrical energy storage and CO_2 capture”. International Journal of Energy Research, Vol. 235, p.1128-1167.

Meireles, T., 2020, *Acordo de Paris completa cinco anos com lições aprendida*, https://www.wwf.org.br/?77471/Acordo-de-Paris-completa-cinco-anos-com-licoes-aprendidas. Accessed 11 April 2022.

Yu, H., Gundersen, T. and Gençer, E, 2021. “Optimal liquefied natural gas (LNG) cold energy utilization in an Allam cycle power plant with carbon capture and storage”. *Energy Conversion and Management*, Vol. 228.

8. RESPONSIBILITY NOTICE

The authors are the only responsible for the printed material included in this paper.